

**Case Study of a Global Shutter CIS--Part 1
Angular Dependency of the Light Sensitivity**

Theuwissen, Albert

DOI

[10.1109/TED.2022.3165009](https://doi.org/10.1109/TED.2022.3165009)

Publication date

2022

Document Version

Accepted author manuscript

Published in

IEEE Transactions on Electron Devices

Citation (APA)

Theuwissen, A. (2022). Case Study of a Global Shutter CIS--Part 1: Angular Dependency of the Light Sensitivity. *IEEE Transactions on Electron Devices*, 69(6), 2932-2937.
<https://doi.org/10.1109/TED.2022.3165009>

Important note

To cite this publication, please use the final published version (if applicable).
Please check the document version above.

Copyright

Other than for strictly personal use, it is not permitted to download, forward or distribute the text or part of it, without the consent of the author(s) and/or copyright holder(s), unless the work is under an open content license such as Creative Commons.

Takedown policy

Please contact us and provide details if you believe this document breaches copyrights.
We will remove access to the work immediately and investigate your claim.

Case Study of a Global Shutter CIS—Part 1: Angular Dependency of the Light Sensitivity

Albert Theuwissen¹, *Life Fellow, IEEE*

Abstract—This article focuses on the angular dependency of the light sensitivity of a commercially available CMOS camera with a global shutter (storage node (SG) in the charge domain) and shared pixel architecture. The angular dependency is characterized as a function of both the wavelength and the angle of incidence of the incoming light. The measurement results are linked to the layout of the pixels as a means to explain the obtained characterization data.

Index Terms—Angular dependency light sensitivity, CMOS image sensor, global shutter, wavelength dependency.

I. INTRODUCTION

IT IS well known in the solid-state imaging community that the light sensitivity of a solid-state image sensor strongly depends on the angle of incidence of the incoming light. In most cases, the highest possible light sensitivity is obtained for photons perpendicularly arriving to the sensor. What is more, in many cases, the multi-layer structure above the silicon is optimized for maximum photon penetration in the silicon for perpendicularly incoming light. However, as soon as the light rays form a certain angle with the normal, the light sensitivity decreases, and the reduction can be quite drastic.

In this article, the angular light sensitivity of a commercially available global shutter image sensor is measured and analyzed, not only as a function of the angle of the incoming light, but also as a function of the wavelength. As of publication, the latter is not yet sufficiently described in the technical literature.

This article is the first part of a diptych and should be seen as a kind of preparation for the second part, which deals with parasitic light sensitivity. But in the meantime, some interesting characteristics can already be revealed here.

II. SENSOR ARCHITECTURE

A commercially available USB-3 camera is used in the analysis. The architecture of the monochrome global shutter CMOS image sensor is based on a charge-domain storage node (SG). The pixel has a standard four-transistor configuration with a pinned photodiode and a “standard” output structure

Manuscript received December 20, 2021; revised February 25, 2022; accepted March 26, 2022. The review of this article was arranged by Editor R. Kuroda.

The author is with Harvest Imaging, 3960 Bree, Belgium, and also with the Delft University of Technology, 2628 CD Delft, Netherlands (e-mail: albert@harvestimaging.com).

Color versions of one or more figures in this article are available at <https://doi.org/10.1109/TED.2022.3165009>.

Digital Object Identifier 10.1109/TED.2022.3165009

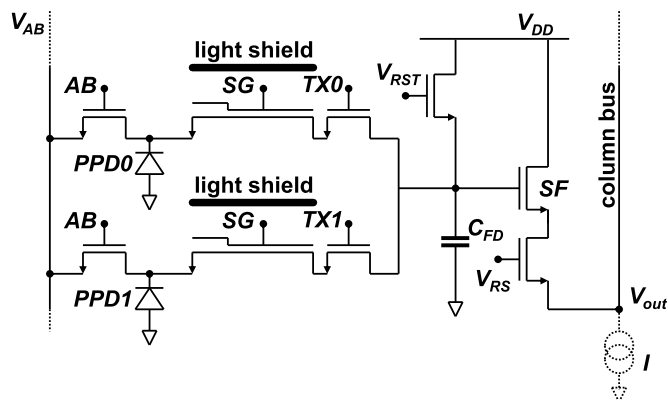


Fig. 1. Pixel architecture present in the device being tested, based on a $2V \times 1H$ shared pixel with a global shutter SG in the charge domain.

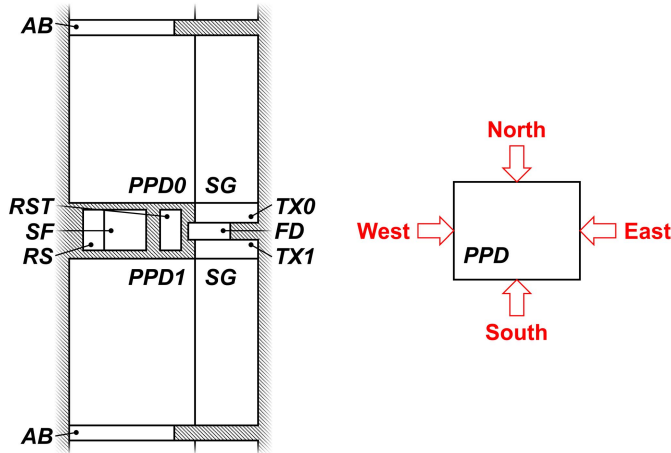
[reset transistor (RST), select transistor (RS), and source follower (SF)] for two photodiodes (PPD0 and PPD1). The pixel architecture is shown in Fig. 1.

Additional features to the well-known four-transistor or 4T pixel are as follows [1].

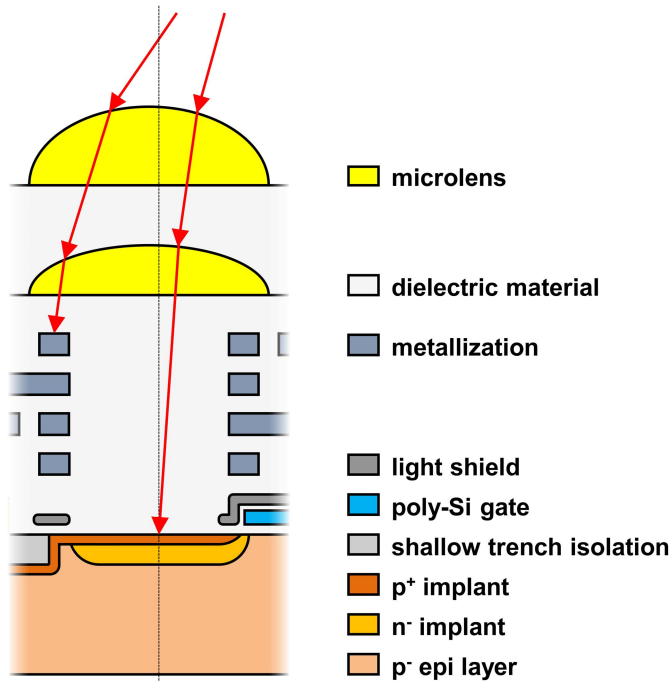
- 1) Two photodiodes (and thus two pixels) which share the readout amplifier (reset, SF, row select) as well as control the anti-blooming (AB) transistor and control the SGs. The two pixels sharing the readout structure belong to adjacent rows and have the column bus in common.
- 2) An AB transistor per pixel to prevent blooming artifacts in the case of overexposure. These AB transistors can also be used to globally empty the photodiodes at the beginning of an exposure. The latter effect can also be realized by activating the SG and TX0/TX1 gates.
- 3) An SG between the photodiodes (PPD0 and PPD1) and an SF to act as the in-pixel memory node necessary to operate the device with a global shutter. What is important to notice is the presence of a light shield above the SG that prevents that light from penetrating into the SG.

The timing of the device follows the subsequent sequence during the capturing of an image.

- 1) All pixels are reset by a global operation of the AB transistor: all charges present in the pinned photodiodes (PPD0 and PPD1) are drained to the AB node biased at a high voltage.
- 2) All pixels are exposed at exactly the same exposure time to the incoming light (= both the start as well as the end



(a)



(b)

Fig. 2. (a) Layout of the $2V \times 1H$ shared pixel of the device being tested (the illustration is based on the SEM photographs provided by TechInsights; there is a small chance that in reality the pixels are rotated over 180° and/or mirrored around a vertical axis). (b) “Best guess” of the cross section of the pixel.

of the exposure time are equal for all pixels, globally defined).

- 3) At the end of the exposure, the charges (electrons) present in the pinned photodiodes PPD0 and PPD1 are transferred all at the same time to the SGs by pulsing the SG gates. This global action is a fundamental requirement of a global shutter device.
- 4) After the exposure, the readout of the information from the SGs is initiated by means of the transfer gates (TX0 and TX1). A positive pulse on these transfer gates moves the charges to the floating diffusion capacitor (C_{FD}), where the charge packet is converted to a voltage.

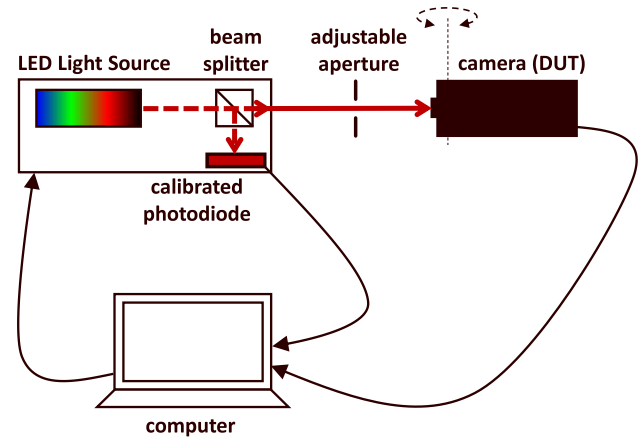


Fig. 3. Sketch of the measurement setup.

The latter in turn is read out through the SF. This readout of the image is based on a row-after-row readout sequence.

III. LAYOUT OF THE PIXELS

The layout of the shared pixels is sketched in Fig. 2(a) (not drawn to scale). The pixel size is $3.45 \mu\text{m}$, the pixels are provided with microlenses to increase the fill factor [2].

One detail present in the layout that can play an important role in the discussion of the angular dependency of the light sensitivity: the photodiodes PPD0 and PPD1 are not perfectly equal to each other. For instance, the top side of PPD0 is defined by the AB gate and device isolation, while the bottom side of PPD0 is only defined by device isolation. For PPD1, the top and bottom definitions are reversed compared to PPD0. This asymmetry can have a negative effect on the opto-electrical characteristics. On the other hand, the definition of PPD0 and PPD1 at their left side or at their right side is the same. A “best guess” cross section of the pixels is illustrated in Fig. 2(b) (not drawn to scale).

Fig. 2(b) illustrates the cross section from left to right of PPD0 and PPD1, so that the poly-Si gate resembles the storage gate SG. But the illustration also parallels the cross section from the bottom to the top of PPD0, or from the top to the bottom of PPD1 (PPD0 and PPD1 are mirrored along a horizontal axis, so what is top for PPD0 is bottom for PPD1, and vice versa). Both cases begin with a shallow trench isolation region as the device isolation, after which the pinned photodiode is present and is bound by the AB gate at the opposite side. As depicted in Fig. 2(b), the light shield is overlapping the photodiode, the overlap is estimated to be, respectively, $0.5 \mu\text{m}$ along the storage gate side SG, $0.3 \mu\text{m}$ at the opposite side of the storage gate SG, $0.15 \mu\text{m}$ along the AB gate and $0.25 \mu\text{m}$ at the opposite side of the AB gate, the opening of the lightshield above the photodiode is $1.1 \mu\text{m} \times 1.7 \mu\text{m}$ (these numbers are based on results obtained after deprocessing).

Thus, in theory, because the sensor is using two (slightly) different photodiodes, the characterization of the angular dependency has to be considered for the two cases, and the

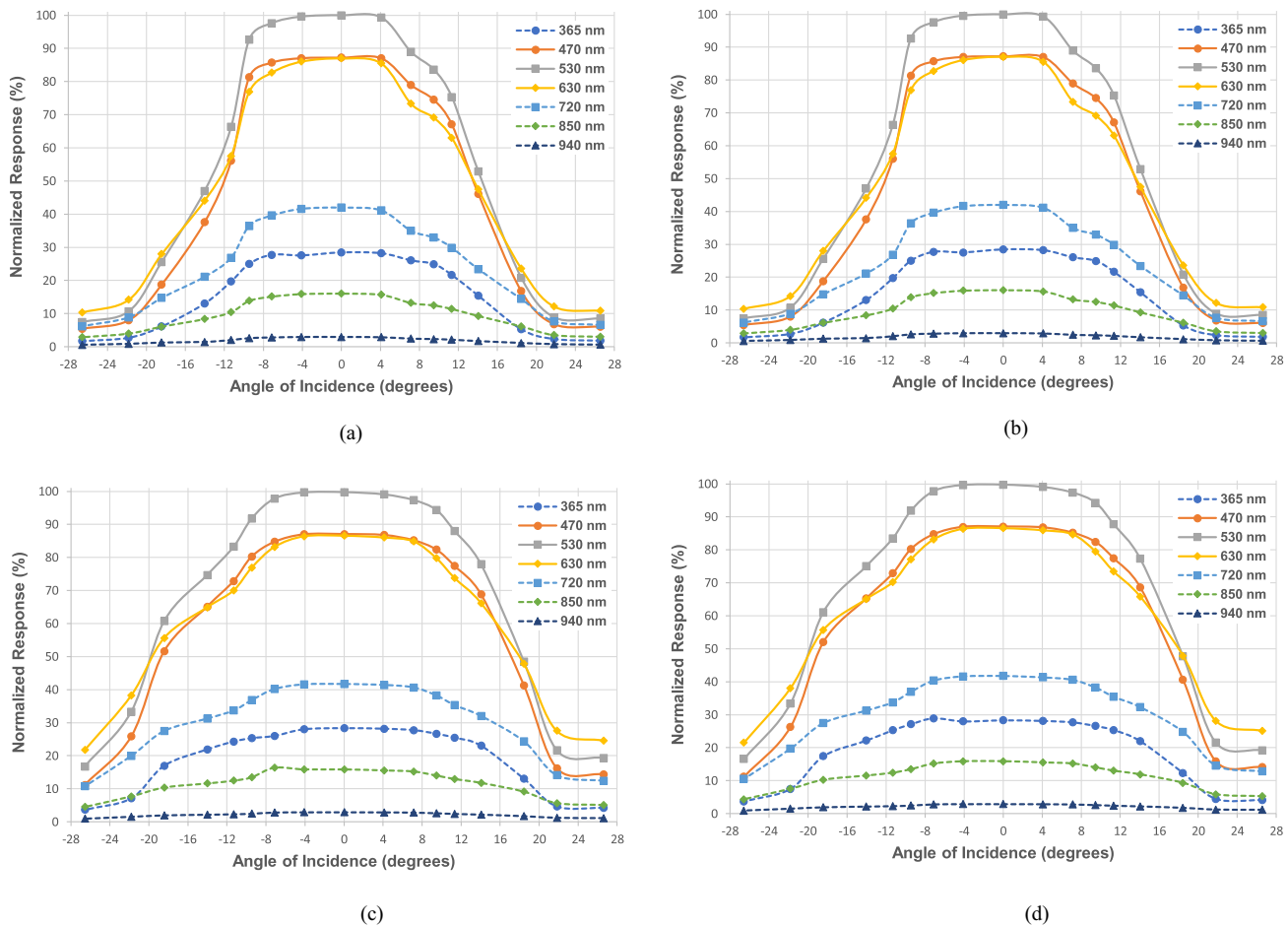


Fig. 4. (a) Angular dependency of the pixels belonging to the even rows (pixel 0) as a function of the incoming angle (positive value: east direction; negative value: west direction), with the wavelength of the incoming light as a parameter. (b) Angular dependency of the pixels of the odd rows (pixel 1) as a function of the incoming angle (positive value: east direction; negative value: west direction), with the wavelength of the incoming light as a parameter. (c) Angular dependency of the pixels belonging to the even rows (pixel 0) as a function of the incoming angle (positive value: north direction; negative value: south direction), with the wavelength of the incoming light as a parameter. (d) Angular dependency of the pixels of the odd rows (pixel 1) as a function of the incoming angle (positive value: north direction; negative value: south direction), with the wavelength of the incoming light as a parameter.

four directions (as indicated in Fig. 2(a) as well): north, south, east, and west.

IV. MEASUREMENT METHOD

For the measurement of the angular dependency of the light sensitivity, the sensor is operated in standard global shutter mode (without lens attached) as defined by the camera supplier. The characterization setup is shown in Fig. 3. A commercially available LED-based light source is used with a built-in, calibrated photodiode to measure the light intensity. The camera can rotate clockwise and anti-clockwise around a vertical axis that goes through the center of the image sensor. (To allow rotation around a horizontal axis, the camera itself is rotated over 90° .) Between the output of the light source and the sensor, an adjustable aperture is placed to minimize any influence of stray light. Moreover, the complete setup (except the computer) is placed in a light-tight box. During the measurements, the exposure time of the uniform illumination being captured is adjusted so that the sensor reaches about 75% of its saturation value. Assuring

the sensor has a quasi-constant output level for the various measurements will avoid issues with saturation and linearity. Next, the following data is recorded:

- 1) exposure time (μs), which is software defined;
- 2) light intensity ($\mu\text{W}/\text{cm}^2$), which is measured by a calibrated photodiode present in the light source; and
- 3) output signal (DN) of the sensor.

From the obtained data, the output signal generated in the pixel per $\mu\text{W}/\text{cm}^2$ light input and per μs exposure time can be calculated (= active signal).

All measurements are conducted as follows.

- 1) As a function of wavelength of the incoming signal. The light source used is based on multiple LEDs of various wavelengths: 365, 470, 530, 630, 720, 850, and 940 nm, of which the amount of light output can be digitally regulated. The full-width half-max (FWHM) values for the various LEDs are, respectively, 8.8, 18.9, 31.1, 13.1, 25.8, 20.7, 38.3, and 70.8 nm.
- 2) As a function of the angle of incidence of the incoming light (0° , 4.1° , 7.1° , 9.5° , 11.3° , 14.1° , 18.4° , 21.8° ,

26.6°), these fixed angles are defined by a kind of a mold in which the camera is fixed during the measurements in all four directions (north, south, east, west).

3) At room temperature.

V. ANGULAR DEPENDENCY RESULTS

To characterize the angular dependency, the active signal is measured. All data obtained from the measurements are normalized (afterward during the data processing) to an input light power of $25 \mu\text{W}/\text{cm}^2$ and an exposure time of $1.00 \mu\text{s}$.

The active light signal for the four directions, as a function of the angle of incidence, are shown in Fig. 4(a)–(d). The parameter used in all graphs is the wavelength of the incoming light; all results are normalized to the largest signal obtained in all measurements.

It can be expected that the light sensitivity would be a significant function of the angle of incidence [3], because the pixels have a limited fill factor, as can be seen in Fig. 2(b). The latter is artificially increased by one microlens, or in the case of the device being tested, by two microlenses placed above each other. The incoming light falling on the microlenses, which cover almost 100% of the pixel area, has to be focused on the photodiodes with an area much smaller than 100% of the pixel area. This focusing effect strongly depends on the angle of incidence. If the angle of the incoming light deviates too much from the normal, the light will no longer be (completely) focused on the underlying photodiode. This effect can drastically decrease the light sensitivity depending on the angle of incidence [4], [5].

A very similar effect can occur at the edges of the image sensor, where the angle of light by definition is not perpendicular to the microlenses. It is, therefore, not surprising that when there is a light fall-off from the pixels, which depends on the pixel location, the light sensitivity will decrease close to the edges of the image sensor. All these angular dependencies can be influenced by the F-number of the lens. High F-numbers result in more collimated light, whereas low F-numbers result in light that arrives at the pixels at different angles. But in all measurements reported in this article, the camera is used without a main lens and with collimated light.

Fig. 4(a) and (b) shows the angular dependency for the east–west direction (east positive value on the horizontal axis; west negative value on the horizontal axis). The curves are not symmetric, indicating a different angular dependency for light coming from the east and from the west direction. The response fall-off for incoming light from the east direction occurs at a larger angle than it does for incoming light from the west direction. This effect can be explained by means of the side walls (left and right) of the pixels, which are not the same for both sides. At the left side of the pixels, light coming from the east direction hits a stack of metal buried in dielectric layers; at the right side of the pixels, light coming from the west direction hits a different stack of metal buried in dielectric layers as well as a higher side wall of the light shield above the SG. On the other hand, this light shield can also create a kind of shadow for light coming from the east side; this shadow effect is less pronounced for light coming from the west side. Not only the structure above the silicon is different for the left

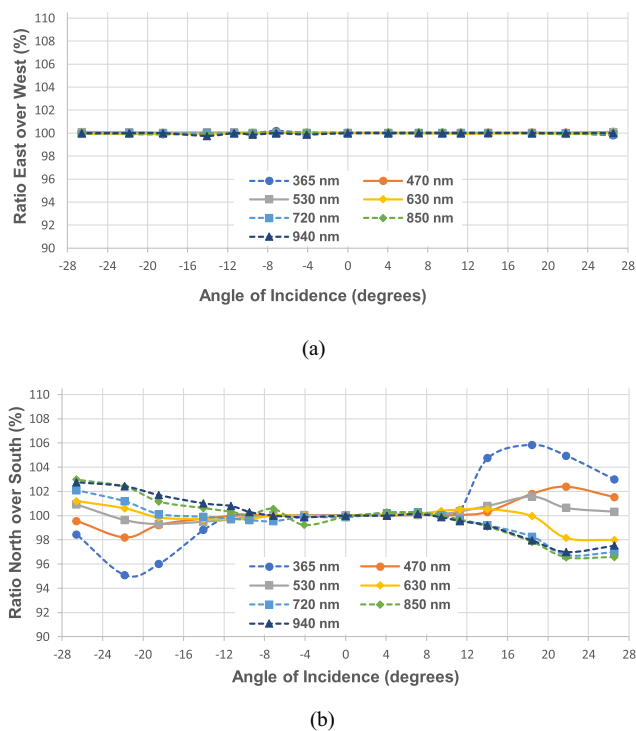


Fig. 5. (a) Ratio of the light sensitivity of odd and even pixels, as a function of the angle of incidence (positive value: east direction; negative value: west direction), with the wavelength of the incoming light as a parameter. (b) Ratio of the light sensitivity of odd and even pixels, as a function of the angle of incidence (positive value: north direction; negative value: south direction), with the wavelength of the incoming light as a parameter.

and right sides of the photodiodes, but also the structure in the silicon will be different. This can create a non-uniformity in crosstalk that the pixels encounter when the light is coming from the east or the west side.

Fig. 4(c) and (d) shows the angular dependency for the north–south direction (north positive value on the horizontal axis; south negative value on the horizontal axis). The curves are not symmetric, indicating a different angular dependency for light coming from the north and from the south direction. The response fall-off for incoming light from the north direction occurs at a larger angle than it does for incoming light from the south direction.

This effect can again be explained by means of the side walls (top and bottom) of the pixels, which are not the same for both sides. At the top side of the pixels, light coming from the south direction hits a stack of metal buried in dielectric layers; at the bottom side of the pixels, light coming from the north direction hits a different stack of metal buried in dielectric layers. Besides the differences in pixel architecture on top of the silicon, also the pixels have a different structure inside the silicon. Consequently, variations in crosstalk can also result in nonsymmetric angular dependency curves.

The asymmetry for the north–south results is smaller than the asymmetry for the east–west results. Also, the curves in Fig. 4(c) and (d) are wider than those in Fig. 4(a) and (b). This effect can be explained by the size of the photodiodes, which are larger in the vertical direction (north–south) than in the horizontal directions (east–west), as sketched in Fig. 2(a).

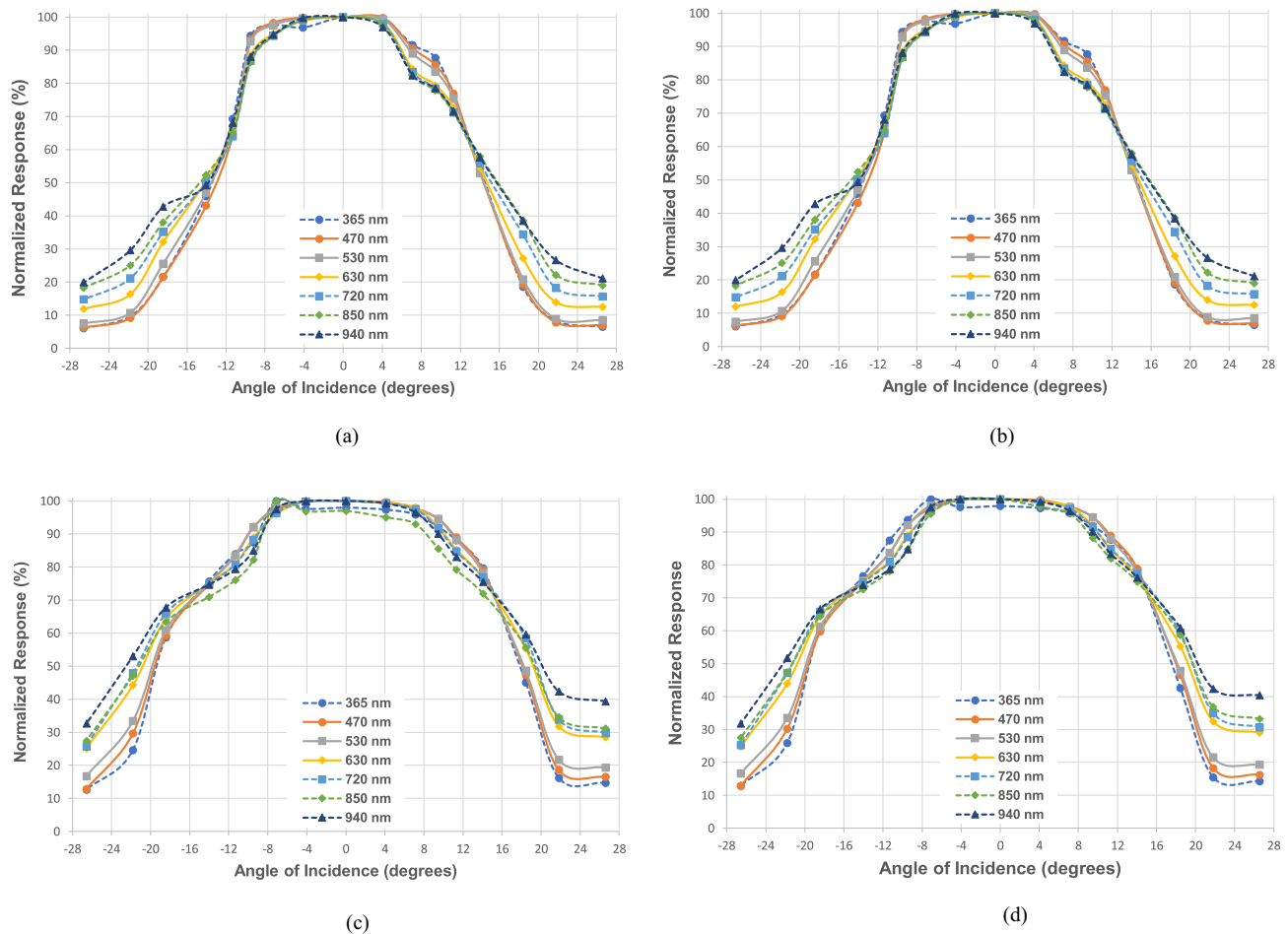


Fig. 6. (a) Angular dependency of the pixels belonging to the even rows (pixel 0) as a function of the incoming angle (positive value: east direction; negative value: west direction), with the wavelength of the incoming light as a parameter. (b) Angular dependency of the pixels of the odd rows (pixel 1) as a function of the incoming angle (positive value: east direction; negative value: west direction), with the wavelength of the incoming light as a parameter. (c) Angular dependency of the pixels belonging to the even rows (pixel 0) as a function of the incoming angle (positive value: north direction; negative value: south direction), with the wavelength of the incoming light as a parameter. (d) Angular dependency of the pixels of the odd rows (pixel 1) as a function of the incoming angle (positive value: north direction; negative value: south direction), with the wavelength of the incoming light as a parameter.

What is valid for all four curves in Fig. 4 series is: they all reach their maximum for perpendicularly incoming light.

To further investigate any differences between odd and even pixels, Fig. 4(a) and (b) need to be compared to each other, as well as Fig. 4(c) and (d). The calculated ratios of all the obtained curves and data in Fig. 4(a) and (b) are illustrated in Fig. 5(a).

As can be seen, all results are equal to or at least very close to 1. This indicates that there are no differences in angular dependency between odd and even pixels for light that is coming from the east or the west direction. This conclusion can be expected because the pixels are perfectly identical in the horizontal direction. Comparing Fig. 4(c) and (b), and calculating the ratios of the curves and data obtained in these two figures gives the result shown in Fig. 5(b).

Although most ratios of the light sensitivities come close to 1, some curves deviate from this ideal value. Especially, the non-visible wavelengths tend to do worse than the visible

wavelengths. Although the image sensor used is a monochrome device intended for machine vision application, it can be mentioned that for consumer color applications, the aforementioned effect is a positive observation. But for applications in the near infrared, the unequal light sensitivity of odd and even pixels can lead to the necessity of extra fixed-pattern noise corrections.

Another very interesting observation can be made: a few curves show some mirror-symmetry around the 0° point of the curves. For instance, the curves of 850 and 720 nm have a ratio larger than 100% for negative angles, while the ratio is smaller than 100% for positive angles. The opposite is true for the curves of 365, 470, and 530 nm. This effect is due to the mirrored (around a horizontal axis) layout of the even and odd pixels (= the top side of the PPD0 is the same as the bottom part of the PPD1 and vice versa) as is shown in Fig. 2(a).

In Fig. 6(a)–(d), the angular dependency is presented like it was in Fig. 4(a)–(d).

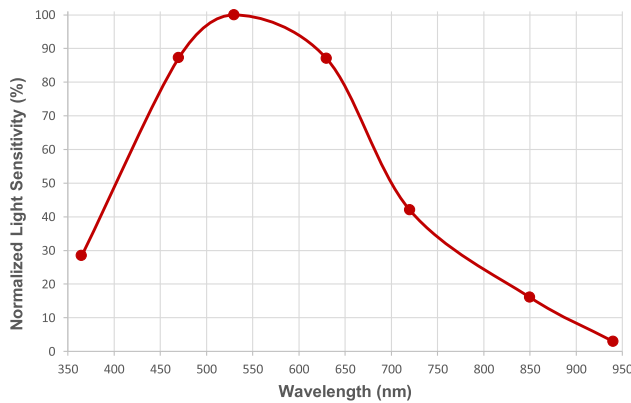


Fig. 7. Normalized light sensitivity as a function of wavelength for perpendicularly incoming light and for light with $25 \mu\text{W}/\text{cm}^2$ of power.

The difference between the two sets of figures is: in Fig. 4 series, the information is normalized to the largest signal in all measurements, whereas in Fig. 6 series, the information obtained for each wavelength is normalized to the largest signal for that particular wavelength. In this way, the shape of the obtained curves and the stability of the color ratio can be checked.

Based on Fig. 6(a)–(d), the conclusion can be made that the angular dependency is becoming worse for shorter wavelengths of the incoming light (although the variation across the visible and near-IR spectrum is not that large), especially for larger angles of incidence. For smaller angles of incidence, this effect is not always present. A possible explanation for the lower light response for shorter wavelengths (in combination with larger angles of incidence) can be found in an increased reflection of incoming photons. The refractive index of the silicon substrate depends on the wavelength of the incoming light (becomes larger for shorter wavelengths) and so does the amount of reflected light for shorter wavelengths.

In Fig. 6(a) and (b), two groups of curves can be recognized: the wavelengths 365, 470, and 530 nm behave very much the same, as well as the wavelengths 630, 720, 850, and 940 nm. There is no direct explanation for this division in two groups. This grouping effect is not visible in Fig. 6(c) and (d).

The curves in Fig. 6 series give an indication of how well the color ratio (e.g., B/G and R/G) can be maintained depending on the wavelength and angle of incidence. Small changes in the color ratio can result in color fringing in real color images, and the need for extra corrections in the color pipeline processing. Remarkably, all wavelengths fall on top of each other at an angle between 8° and 12° .

VI. LIGHT SENSITIVITY RESULTS

Although initially not the main priority of this research project, the light sensitivity as a function of the wavelength is

also measured. The result is illustrated in Fig. 7, where the sensor (relative) output is shown as a function of the wavelength of the incoming light. All measurement points represent incoming light at $25 \mu\text{W}/\text{cm}^2$ of power and a perpendicularly incoming light signal.

VII. CONCLUSION

The article describes the results obtained from an angular dependency analysis of a commercially available global shutter CMOS image sensor/camera. The observations can be summarized as follows.

- 1) Due to the shared pixel architecture, pixels belonging to odd rows and pixels belonging to even rows show different angular dependency in terms of light sensitivity. This effect can result in a row-wise light fixed-pattern noise.
- 2) Due to the asymmetric pixel layout (in the vertical as well as in the horizontal direction), the angular dependency of the light sensitivity is different for the east and west directions, as well as for the north and south directions. This effect can result in different color fringing effects in the vertical and horizontal directions.
- 3) Due to the rectangular shape of the pixels, the curves obtained from the north–south analysis are wider than the curves obtained from the east–west analysis. Especially, in situations with a large lens opening (low F-number), extra differences in the vertical and horizontal light sensitivity can cause color shifts.
- 4) Due to the high optical stack, the widths of the angular dependency curves are relatively small and the slopes of the curves are relatively steep.

ACKNOWLEDGMENT

The author would like to thank TechInsights for their assistance and support in describing the pixel layout and pixel cross section. Thanks to Sarah, Adri, René, and René for proofreading the manuscript.

REFERENCES

- [1] M. Sakakibara *et al.*, “An 83dB-dynamic-range single-exposure global-shutter CMOS image sensor with in-pixel dual storage,” in *IEEE ISSCC Dig. Tech. Papers*, Feb. 2012, pp. 380–382, doi: [10.1109/ISSCC.2012.6177058](https://doi.org/10.1109/ISSCC.2012.6177058).
- [2] Ray Fontaine TechInsights: Private Communication, Jun. 2021.
- [3] Data Sheet of the KAC12040. *Device Performance Specification*. Accessed: Dec. 20, 2021. [Online]. Available: <https://www.datasheets360.com/pdf/7094393965430832013?query=KAC12040&pqid=115074701>, visited
- [4] T. Yokoyama, M. Tsutsui, Y. Nishi, I. Mizuno, V. Dmitry, and A. Lahav, “High performance $2.5\mu\text{m}$ global shutter pixel with new designed light-pipe structure,” in *IEDM Tech. Dig.*, Dec. 2018, p. 10, doi: [10.1109/IEDM.2018.8614569](https://doi.org/10.1109/IEDM.2018.8614569).
- [5] Y.-W. Cheng, T.-H. Tsai, C.-H. Chou, K.-C. Lee, H.-C. Chen, and Y.-L. Hsu, “Optical performance study of BSI image sensor with stacked grid structure,” in *IEDM Tech. Dig.*, Dec. 2015, p. 30, doi: [10.1109/IEDM.2015.7409801](https://doi.org/10.1109/IEDM.2015.7409801).